MULTIVARIABLE CONTROLLER DESIGN FOR A TRIMMABLE HORIZONTAL STABILIZER ACTUATOR WITH TWO PRIMARY LOAD PATHS

Nils Wachendorf, Frank Thielecke, Udo Carl, Timo Pe
Hamburg University of Technology, Institute of Aircraft Systems Engineering

Keywords: *THSA, H_∞ Controller Design, Mixed Sensitivity Design*

Abstract

A novel drive concept for the Trimmable Horizontal Stabilizer Actuator (THSA) is based on two ballscrews operating in parallel which move the stabilizer to adjust the angle of attack of the horizontal tailplane. The positions of the ballscrew nuts are mechanically synchronized because the two installed differential gearboxes uniformly distribute the mechanical power to the two drive chains independently of the operational condition. A H_∞ controller design is employed to control the rotational speed of the hydraulic motors. The resulting multivariable speed controller is implemented into the nonlinear simulation model, the simulation results of which are validated through measurements at the THSA test rig. The simulation results of the multivariable closed loop are compared with the results obtained from a closed loop with cascade structure.

1 Introduction

The pitch trim of transport aircraft is usually controlled by an adjustable horizontal tailplane. As prescribed by the airworthiness requirements, all safety critical load bearing components of a civil transport airplane are designed to have two independent mechanical load paths. Thus, there must exist two mechanical load paths between the horizontal tailplane and the aircrafts fuselage structure. Today's Trimmable Horizontal Stabilizer Actuator uses in normal operation only one load path (e.g. one ballscrew). In case of failure (disconnection of the first load path/ballscrew) the secondary load path (e.g. a tie rod, which is integrated in the hollow ballscrew) prevents a complete disconnection and an uncontrolled movement of the horizontal stabilizer. Consequently, the second load path is normally unloaded. Compared to a conventional THSA architecture, the concept presented here incorporates two active-parallel operating load paths to move the stabilizer (cp. figure 1). Active-parallel in this case means the appearing airload is shared between the two ballscrew actuators. These comprise single load path ballscrew actuators (BS), displacing the trimmable horizontal stabilizer (THS). The actuation system consists of two differential gearboxes with three shafts each. The arrangement and the mechanical coupling of the two differential gears ensure a synchronization of the two drive chains. Each ballscrew is connected to the planet carrier shaft of a differential gearbox (DG). One input shaft of the differential gearbox is mounted to a variable displacement hydraulic motor (VDHM). The remaining inputs of the differential gearboxes are connected by a so-called cross shaft (CS). This arrangement enables an auto-synchronization of the ballscrew positions precluding force-fight. The two ballscrew nuts are mechanically coupled through the supporting elements of the horizontal stabilizer. Owing to the stationary gear ratio of the differential gears and the sum of moments at the shafts of the differential gearboxes, a torque difference between the two drive chains will be compensated

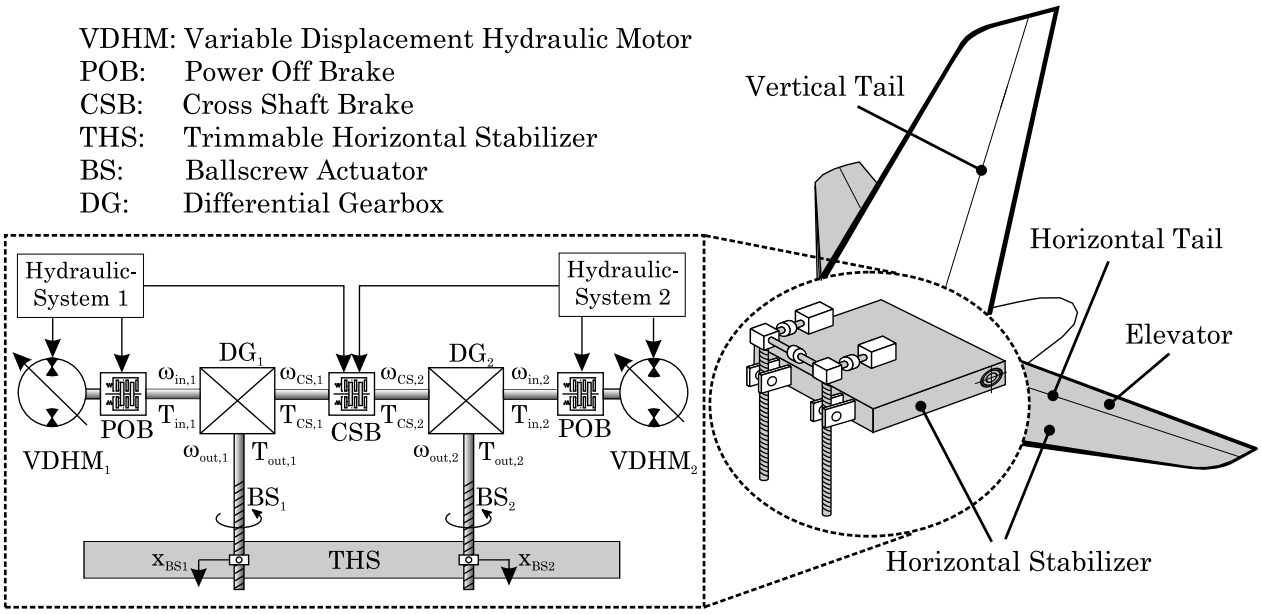

Fig. 1 Trimmable Horizontal Stabilizer Actuator system with two primary load paths

by the cross shaft, which rotates until the torque difference is disposed. In case of symmetrical ballscrew loads, meaning that both planet carrier shafts are affected by identical torques, the cross shaft carries a torque but does not rotate. In order to avoid an uncontrolled movement of the control surface, in case of failure three hydraulic power off brakes (POB) lock the trimmable tailplane in position.

The advantages of this concept, in comparison to conventional systems, is the testability of the mechanical integrity of the two load paths without the need for additional tools, significantly reducing maintenance effort. The mechanical integrity of the drive chains can be checked by activating one motor brake, while driving the system with the second hydraulic motor. In case of a faultless mechanical system, the motor can only rotate a torque and stiffness defined angle. Additionally, mechanical wear on the ballscrews is reduced because of the load-share between the two load paths. Owing to the separation of the load paths, complex components like fail-safe designed gearboxes or a no-back brake are no longer required.

This paper gives an approach for a H_∞ design, controlling the THSA motor speed, is given. In contrast to the well-known decentralized cascade controller design, here one controller for both drive chains is detailed. The controller is computed with the help of the mixed sensitivity method.

The conventional cascade controller architecture for the THSA system includes three convoluted control loops. The rotational speed of the hydraulic motor is controlled by a PI controller with subordinated position control of the swashplate. The stabilizer position is controlled by a proportional controller for the angular position of the ballscrew. Thus, the control system for the THSA consist of a cascade with three convoluted control loops, each for one drive chain. This cascade structure will consequently be replaced by a multivariable controller.

To avoid bending stresses at the mechanical coupling device of the two nuts, the multivariable feedback controller design represents a control system solution to synchronize the motor speeds, so that both ballscrew nut positions are identical. In case of failure (e.g. 1-motor operation) the mechanical self-synchronization assures a force fight free moving of both ballscrew actuators. In order to achieve a self-contained controller design and to synchronize both drive chains, a mul-

tivariable system (MIMO) approach is chosen.

The obtained controller is implemented into the nonlinear simulation model and simulation results are compared to the cascade controller architecture. The simulations are validated by measurements at the THSA test rig, which was set up at the Institute of Aircraft Systems Engineering.

2 THSA System Structure

In order to explain the mechanical interaction between the two drive chains, the main elements of the actuation concept have to be specified. To understand the general actuation system behavior and to get an overview of the dynamic interactions, the differential gears are explained in detail. One gear consists of two large gear rings which are attached to the input shafts. The two gear rings are mechanically coupled by three pairs of planetary wheels meshing with the internal teeth of the ring gear. The planetary wheels are mounted to a carrier (planet-wheel carrier) which is directly coupled to the planet carrier shaft. The main speed- and torque equations are explained in the following.

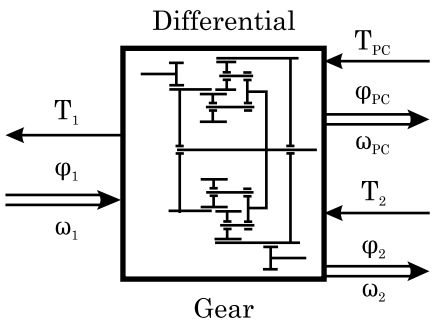

Fig. 2 Schematic of a differential gear

2.1 Basic Kinematic Equations of Differential Gears

To understand the kinematic behavior of the two coupled differential gearboxes, it is necessary to look at the two basic equations of a differential gearbox. First, the main rotational speed equation of the three shafts is given by [4]:

$$\omega_1 - i_{12} \cdot \omega_2 - (1 - i_{12}) \cdot \omega_{PC} = 0, \qquad (1)$$

with the speed of the two input shafts ω_1, ω_2 and the planet carrier shaft ω_{PC} (cp. figure 2).

The stationary gear ratio i_{12} completely describes the kinematic of a differential gear with three shafts. The value of i_{12} is defined as the gear ratio between the two input shafts in case of a fixed planet carrier shaft ($w_{PC} = 0$):

$$i_{12} = \left.\frac{\omega_1}{\omega_2}\right|_{\omega_{PC}=0}. \qquad (2)$$

The adaption of the stationary gear ratio directly leads to the second main equation of the differential gear, describing the relation between the two input torques, neglecting friction- and gearing losses:

$$\frac{T_2}{T_1} = -i_{12}. \qquad (3)$$

Taking into account the sum of moments $T_1 + T_2 + T_{PC} = 0$ and equation (3) the torque at the planet carrier shaft is calculated:

$$\frac{T_{PC}}{T_1} = i_{12} - 1. \qquad (4)$$

As can be seen in equations (3) and (4) the torque ratio of a differential gearbox depends only on the stationary gear ratio and not on the rotational speed of the shafts. Hence, the torque ratio is independent of the operating status of the differential gear.

2.2 Mechanical Power Distribution

The kinematic equations of two mechanically coupled differential gears like in the THSA system, are derived in this section. With the stationary gear ratio of $i_{12} = -1$ and an additional transfer gear (i_{SG}) located at the input shafts, the main speed equation of the used differential gearbox is derived (cf. figure 1, cp. equation (1)):

$$\frac{1}{i_{SG}} \cdot \omega_{in,1,2} + \frac{1}{i_{SG}} \cdot \omega_{CS,1,2} - 2 \cdot \omega_{out,1,2} = 0. \qquad (5)$$

Taking into account the mechanical couplings through the cross shaft and through the structure of the horizontal tailplane:

$$\omega_{CS,1} = -\omega_{CS,2}, \qquad \omega_{out,1} = \omega_{out,2}, \qquad (6)$$

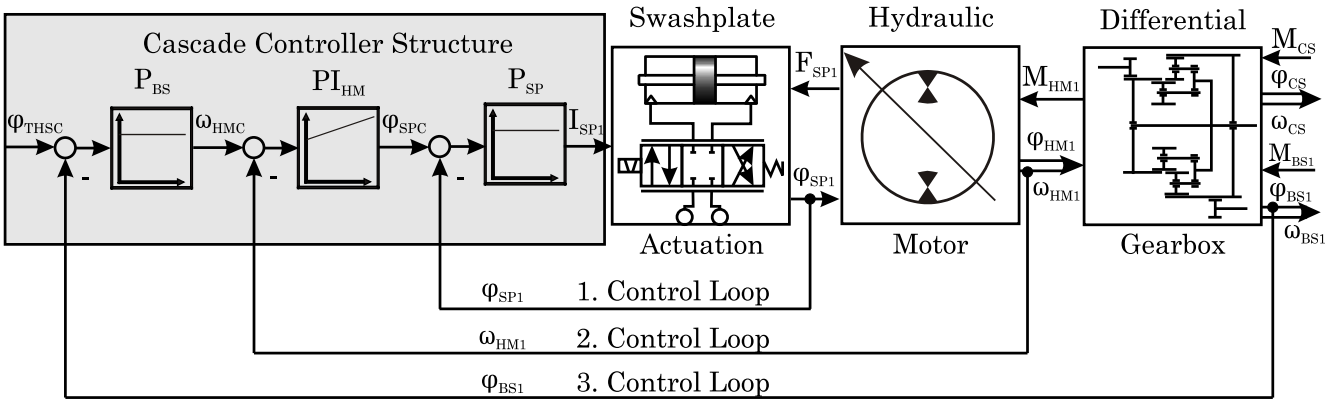

Fig. 3 Cascade controller structure of one drive chain of the THSA system

the superposition of the main speed equation (5) of both differential gearboxes results in:

$$\frac{1}{i_{SG}} \cdot \omega_{in,1} + \frac{1}{i_{SG}} \cdot \omega_{CS,1} - 2 \cdot \omega_{out,1} = \ldots \\ \ldots \frac{1}{i_{SG}} \cdot \omega_{in,2} - \frac{1}{i_{SG}} \cdot \omega_{CS,1} - 2 \cdot \omega_{out,1} \tag{7}$$

$$\Rightarrow 2 \cdot \omega_{CS,1} = \omega_{in,2} - \omega_{in,1}. \tag{8}$$

The result (eqn. (8)) shows that the cross shaft only starts to rotate in case of different motor input speeds. The rotational speed of the planet carrier shaft depends on the motor input speed ω_{in} and the cross shaft speed ω_{CS} (eqn. (5)):

$$\omega_{out} = \frac{1}{2 i_{SG}} \cdot (\omega_{in} + \omega_{CS}). \tag{9}$$

In case of fixed motor shafts, either by no movement commanded or activated power off brakes $\omega_{in} = \omega_{in,1} = \omega_{in,2} = 0$, the cross shaft speed is given by equation (8):

$$\omega_{CS,1} = \omega_{CS,2} = 0. \tag{10}$$

Thus, the mechanical coupling through the cross shaft ensures a fixation of the horizontal stabilizer without using the cross shaft brake.

Using the torque equations (3) and (4) and considering the stationary gear ratio $i_{12} = -1$ and the gear ratio of the spur gear i_{SG}, the torque relations of the THSA are calculated (cf. figure 1):

$$\frac{T_{CS}}{T_{in,1}} = 1, \quad \frac{T_{out,1}}{T_{in,1}} = \frac{T_{out,1}}{T_{CS}} = -2 \cdot i_{SG}. \tag{11}$$

2.3 Cascade Control Concept

The cascade control concept of the THSA is composed out of three stand-alone control loops. The cascade concept is sequently set up of these three loops (cf. figure 3). The first (φ_{SP1}) and the second control loop (ω_{HM1}) are used to control the hydraulic motor rotational speed. The motor torque depends on the displacement volume of the hydraulic motor. The displacement is varied by pivoting the swashplate. The innermost control loop is closed by the measured swashplate angle (φ_{SP1}). To control the motor speed (ω_{HM1}) a second control loop is needed which is closed with a PI controller. The PI controller output signal is used as input signal (ω_{HMC}) for the swashplate angular position control loop. To control the horizontal stabilizer position (φ_{THS}), the third control loop feeds back the angular position of the ballscrew actuator (φ_{BS1}). The output signal of this superior loop is used as input signal (ω_{HMC}) for the motor speed control loop.

The angle of attack of the horizontal stabilizer results from the fixed pitch of the ballscrews and the lever arm of the stabilizer. For each drive chain (motor, gear, shaft transmission ballscrew) a set of three proportional controller gains (P_{BS}, P_{HM}, P_{SP}) and one gain for the integral part of the speed controller (I_{HM}) are evaluated. Therefore, a decentralized control structure is obtained with one stand-alone cascade structure for each drive chain (cp. figure 4). The advantage of

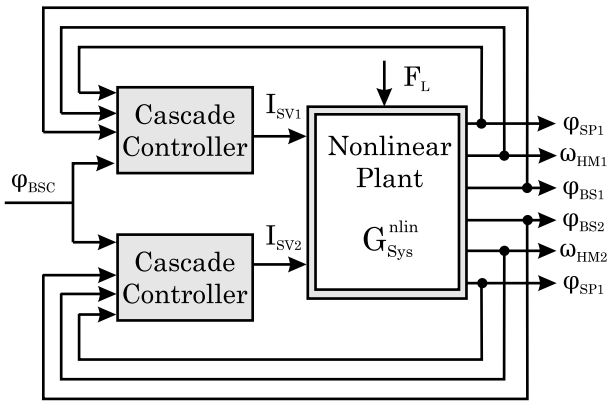

Fig. 4 Decentralized control structure with cascade controller

this cascade control concept is the simple step-by-step calculation of the controller gains by the loop shaping method [2]. This method is adopted to every control loop of the cascade. The closed swashplate position control loop is part of the plant which is used to calculate the PI controller gains of the motor speed control loop. The same method is applied to the ballscrew position control loop [7]. The low order controller is easily implemented into the actuator control electronic.

There are several disadvantages concerning the decentral controller structure. Because of neglecting cross coupling in the controller design, different or varying system parameter in one drive chain (friction, hydraulic pressure, etc.) will lead to different dynamic behavior of the two drive chains, especially in acceleration phases. A further unfavorable aspect of the cascade structure is the inferior performance in case of occurring disturbances (airload is the disturbance input of the plant). The disturbance transfer function is not considered for the cascade controller design. The introduced actuation system structure (two mechanically coupled drive chains) and the above mentioned disadvantages directly lead to a multivariable H_∞ controller design. In anticipation of a better dynamic behavior of the closed loop (little overshoot, short settling time) and little disturbance (airload) sensitivity a H_∞ approach for the THSA system is given in section 4.

3 Test Rig Setup and Measurement Results

In order to verify the presented actuation concept with the mechanical synchronization of the two load paths, a test rig consisting of the already described components was constructed at the Institute of Aircraft Systems Engineering and the set up is pictured in figure 5.

3.1 Actuation System

The main component of the THSA is a so-called power control unit which combines the hydraulic motor (HM), the shaft brakes (POB) and the valve manifold (VM) with the differential gearbox (DG) (cf. figure 5). The hydraulic control elements operating the hydraulic motors and the power off brakes are integrated in the valve manifold. There are four shift valves per manifold; the first two enable the hydraulic pressure, the second two operate the brakes. The swashplate is controlled by a linear hydraulic actuator by means of a servo valve. The whole test rig is operated by a real time DSPACE system (hardware in the loop).

Two of these above mentioned power control units are integrated in the test rig. The planet carrier shaft of each differential gear is connected to one ballscrew (BS) via a shaft transmission (ST). The nuts of the ballscrews in turn are attached to the stabilizer lever (THS) which is pivot-mounted. The two differential gears are coupled through the cross shaft (CS) (see also section 1 and figure 1). There are several items of measurement equipment installed. In addition to the needed sensors for controlling the tailplane position (swashplate angular position, motor speed and ballscrew angular position), the torque and the rotational speed of the planet carrier shafts and the cross shaft are also measured. With the help of the torque and speed signals of the three shafts (planet carrier shafts and cross shaft) the power flow and the power flow direction ($P_{mech} = \omega \cdot T$) through the differential gear can be calculated. Thus, the quality of the mechanical synchronization, depending on friction and gearing losses affecting the cross shaft, is

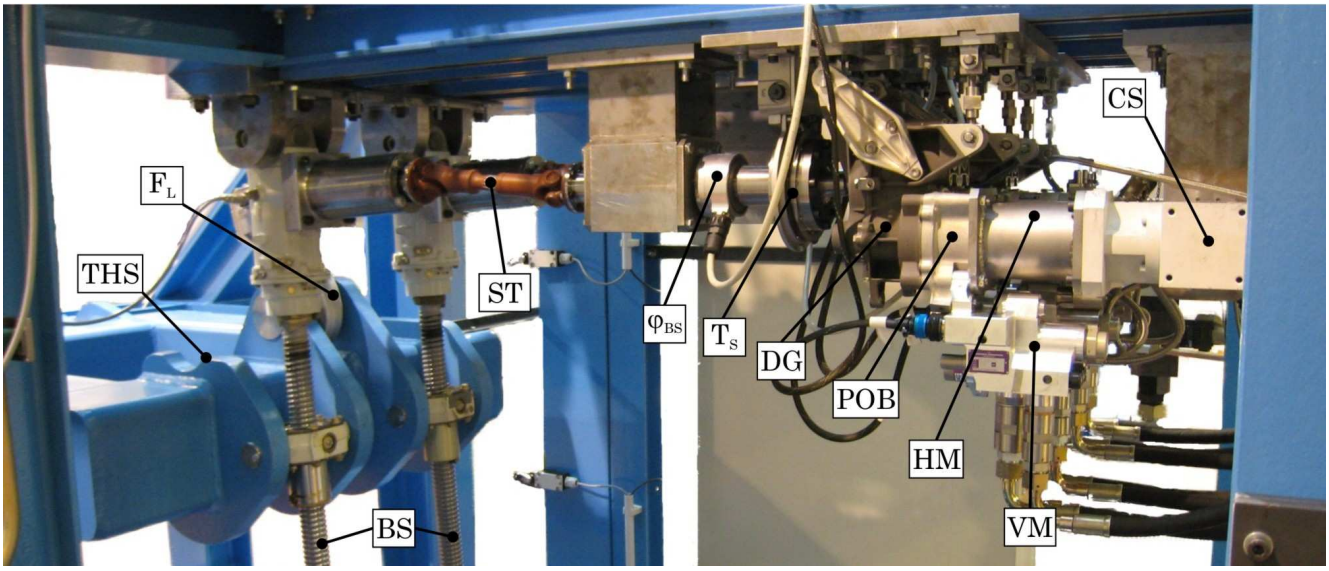

Fig. 5 THSA test rig setup

monitored. The test rig is used to verify simulation results and to prove the new THSA concept in normal operation and in case of failure (pressure loss, motor runaway, jamming).

3.2 Load Simulation

The airload (F_L) affecting the horizontal stabilizer in flight is simulated at the test rig by a linear hydraulic actuator. This actuator is controlled by a servo valve. A load cell is mounted between the actuator and the stabilizer lever in order to close the load simulation control loop. Additionally, a disturbance feedforward is implemented with the lever velocity as input signal to minimize load peaks in case of accelerated motion. The load actuator is able to apply a force of about 220 kN. This load value corresponds to the maximum operating load of the studied original THSA system. Therefore, the new THSA can be tested under operational conditions.

3.3 Comparison of Measurement and Simulation Results of the Cascade Concept

In this section, the complex model including all non-linear components and effects is utilized (e.g. backlash, stiction, saturation effects) to simulate the THSA non-linear dynamic behavior. Simulation (Sim.) and measurement (Mea.) results are plotted in figure 6. The simulated airload is set to a value of 50 kN during the whole simulation/measurement. To detail the interaction between the two drive chains, first both hydraulic motors are started after a time of 0.5 s and are accelerated up to a rotational speed of 300 rad/s. In the first graph of figure 6, the motor speed ω_{HM1}, ω_{HM2} is pictured, in the second the torques affecting the planet carrier shafts T_{PC1}, T_{PC2} are plotted and the third shows the rotational speed of the cross shaft ω_{CS}.

Up to a time of 2 s both motors operate at the same speed. Consequently, the cross shaft does not rotate ($\omega_{CS} = 0$) because of the coupling through the two differential gears with identical stationary gear ratio ($i_{12} = -1$; cp. eqn. (8)). The planet carrier shaft torques T_{PC1}, T_{PC2} are nearly identical in case of both motors running. Hence, the loads are equally shared between the two ballscrews. This effect is also a consequence of the mechanical synchronization via the cross shaft. Little torque differences (e.g. at the acceleration period after 0.5 s) are compensated by a short movement of the cross shaft (cf. figure 6 graph 3 after 0.5 s). The simulation results already show this balance movement at the beginning (0.1 s), because the airload is coupled into

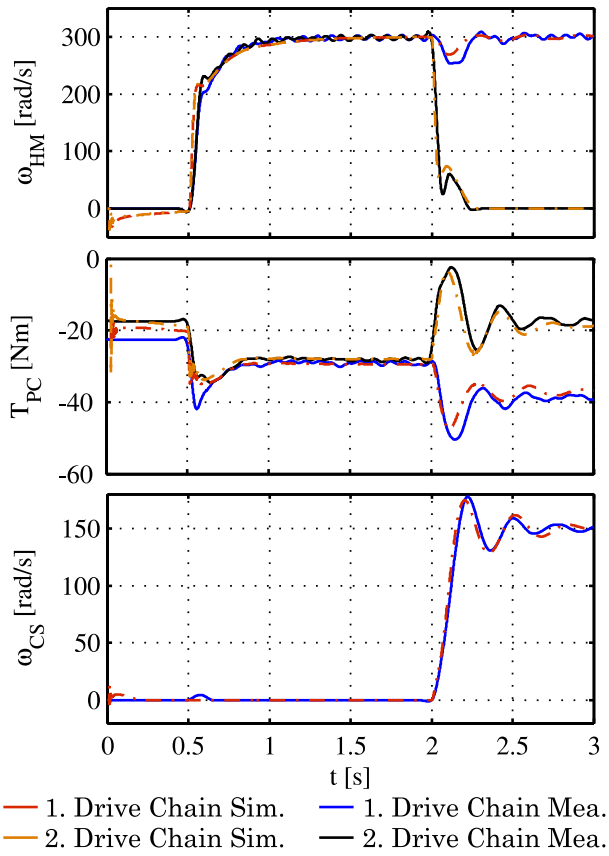

Fig. 6 Hydraulic motor speed ω_{HM}, planet carrier torque T_{PC} and cross shaft speed ω_{CS}

the simulation (commanded step up to 50 kN). After a time of 2 s the speed of the second motor is commanded to zero. Because now only one motor drives the system, the cross shaft starts to turn and transfers half of the provided power to the second drive chain. Consequently, the cross shaft rotates at half of the motor speed. The torque load of the motor is not affected by the speed variation ($i_{12} = -1$ and cp. eqn. (3)), neglecting the friction torque. Therefore, the ballscrews now move only at half speed. The planet carrier torques (T_{PC}) are no longer equal because the torque friction and gearing losses of the differential and the bevel gears, installed at the cross shaft, affect the synchronization. Because the torque friction is dominated by the viscous friction part the torque difference depends on the rotational speed of the cross shaft. An additional influence to the synchronization quality are the gearing losses which mainly depends on the supplied torque. Hence, the torque difference between the two drive chains, in case of different power supply (different motor speeds) depend on the rotational speed of the cross shaft and the value of the applied airload. At the test rig, a maximum torque difference of 20 Nm, (8% of nominal load) between the planet carrier shafts which corresponds to a maximum of mechanical losses of 2.4 Nm at the cross shaft, is not exceeded.

The motor speed cascade controller shows adequate results in simulation as well as in measurement. The commanded motor speed value is reached without any overshoot, but the settling time is about 0.5 s, which is not as fast as desired. A detailed analysis of the speed control loop in case of disturbance (varying airload) and a comparison to the multivariable H_∞ design is given in the following sections.

4 Multivariable Controller Design for the THSA

The decentralized cascade control concept does not account for the cross coupling inherent in the THSA system. Therefore, design requirements like a control system solution for motor speed synchronization cannot be realized with the decentralized concept. By means of the mixed sensitivity design (H_∞ method), a complete controller for the THSA is calculated which can achieve several control system requirements such as little overshoot, short settling time and little disturbance sensitivity. The design method provides, by choosing appropriate weighting matrices, a controller which combines and fulfills the defined specifications. The cross couplings are considered in this design, so that additional demands, like e.g. no cross shaft movement in faultless mode, can be achieved.

4.1 General H_∞ Problem

Quantitative and robustness requirements can be expressed with the help of the frequency dependant singular values of the transfer function. These requirements can be indicated by the so

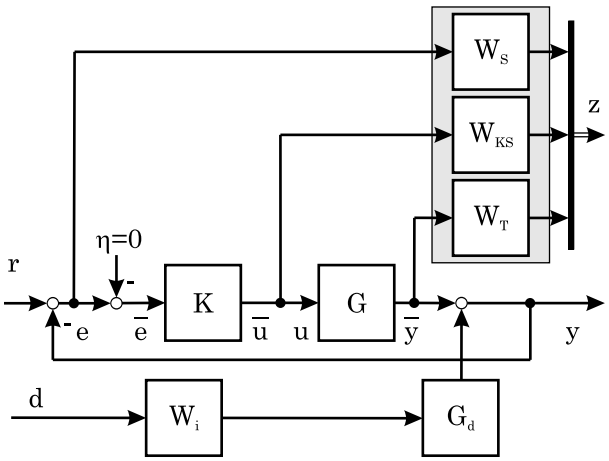

Fig. 7 Generalized plant of the S/KS/T mixed sensitivity problem

called ∞-norm [5]. First of all the L_∞-norm has to be defined: the set of all $p \times q$ field transfer matrices $G(s)$ without poles on the imaginary axis is denoted as $\mathcal{RL}_\infty^{p\times q}$. For every $G \in \mathcal{RL}_\infty^{p\times q}$ the L_∞-norm is given [3]:

$$\|G(s)\|_\infty = \sup_\omega \overline{\sigma}[G(j\omega)]. \tag{12}$$

The L_∞-norm of a transfer function $G(s)$ describes the smallest upper bound of the biggest singular value $\overline{\sigma}[G(j\omega)]$ and can be taken out of the singular value diagram of the related frequency response matrix. The L_∞-norm of a SISO system corresponds to the largest distance of the frequency response locus to the origin in the Nyquist plot. The subset $\mathcal{RH}_\infty^{p\times q}$ contains the set of all realizable asymptotically stable $p \times q$ field transfer matrices. If $G \in \mathcal{RH}_\infty^{p\times q}$ the equation (12) is named H_∞-norm. Several methods exist to calculate the H_∞-norm iteratively [1].

4.2 Mixed Sensitivity Design

The mixed sensitivity problem or S/KS/T problem uses the field transfer matrices S, T and KS for a frequency-dependent weighting of the nominal control loop. The matrices are combined to a functional form which is then minimized over all plant stabilizing controller gain matrices K [6]:

$$\inf_{stab.K} \left\| \begin{pmatrix} W_S S & -W_S S G_d W_i \\ W_{KS} KS & -W_{KS} KS G_d W_i \\ W_T T & -W_T T G_d W_i \end{pmatrix} \right\|_\infty . \tag{13}$$

The choice of W_S, W_{KS}, W_T and W_i influences the values of S, T and KS. The matrix S is called sensitivity and T is the complementary sensitivity matrix. The matrix S describes the sensitivity of the error signal $e = r - y$ relative to the output disturbance and the reference signal. The values of S and T correspond to the quantitative requirements for the controller design: noise elimination, excellent reference action of the control loop. Owing to the relation $S = 1 - T$, the sensitivity matrices have to be chosen $|T(j\omega)| \approx 1$ at low frequencies and $|S(j\omega)| \approx 1$ at high frequencies. The matrix KS specifies the necessary input magnitudes to reach the commanded values.

The generalized plant of the minimizing problem (cp. eqn. (13)) is plotted in figure 7. The signals e, u, $\bar{y}$ of the nominal plant are weighted with the frequency depending matrices W_S, W_{KS} and W_T. The disturbance d is weighted with W_i. The external input values r and d and the external output variables:

$$z = \begin{pmatrix} W_S & 0 & 0 \\ 0 & W_{KS} & 0 \\ 0 & 0 & W_T \end{pmatrix} \begin{pmatrix} e \\ u \\ \bar{y} \end{pmatrix},$$

define a generalized plant, the H_∞-norm of which has to be minimized in our problem. The choice of the weighting matrices W_S, W_{KS} and W_T for the THSA system is explained in detail in the following.

4.3 Controller Design

A multivariable motor speed controller is calculated with the help of the mixed sensitivity design and is implemented into the nonlinear system model. The rotational speed of the first motor (ω_{HM1}) and the difference of the motor speeds $\Delta\omega_{HM} = \omega_{HM1} - \omega_{HM2}$ (cf. figure 8) are chosen as reference signals. This control structure is selected because a possible speed difference, especially in acceleration phases due to varying

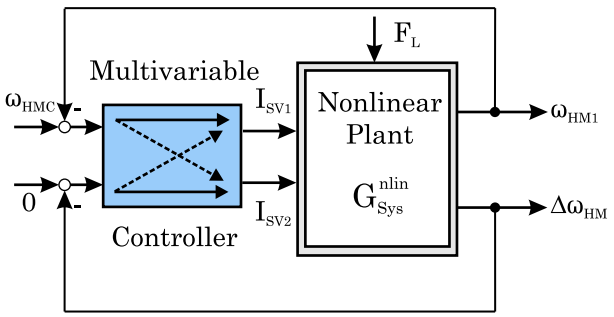

Fig. 8 Control loop structure of the H_∞ approach

system parameters in one drive chain (hydraulic pressure, inertia, friction), will be compensated by a feedback of $\Delta\omega$.

A linear system model of the THSA is designed in order to be able to calculate the generalized plant for the mixed sensitivity design. The linear model is analytically set up to minimize rounding errors especially when calculating the observability and controllability of the system. The THSA is fully controllable and all signals needed for the control loop are measured. Furthermore, the analytical linear model is used to identify the model uncertainties with significant influence on the dynamic behavior. This information is used in a continuative robust controller design with norm bounded uncertainties. For the controller design, a full rank approach is realized with a first order low pass filter characteristic of the weighting matrix W_S:

$$W_S = \frac{\frac{s}{M_{S,i}} + \omega_{S,i}}{s + \omega_{S,i} \cdot \varepsilon_{S,i}} \cdot I, \text{ with } i = 1, \ldots, n, \quad (14)$$

and a first order high pass filter characteristic of W_T [8]:

$$W_T = \frac{s + \frac{\omega_{T,i}}{M_{T,i}}}{s \cdot \varepsilon_{T,i} + \omega_{T,i}} \cdot I, \text{ with } i = 1, \ldots, n, \quad (15)$$

The weighting matrix KS is not used for the controller design presented in here. The disturbance rejection matrix W_i is set up as a simple gain ($W_i = \delta \cdot I$). As there are two inputs and two outputs to the controller, the order n of the weighting matrices S and T is two. The disturbance input is only scalar. The mixed sensitivity problem is solved with standard software (MATLAB ROBUST CONTROL TOOLBOX; 2-Riccati solution). The singular values σ_1 and σ_2 of S/KS/T of the calculated controller are plotted in figure 9. The boundaries, influenced by the weighting matrices, are represented by orange and black lines in figure 9. The singular values are normalized by the maximum amplitude of the control variables. The singular values of the sensitivity and complementary sensitivity function do not exceed the given boundaries. The control sensitivity raises up to $+20\,\mathrm{dB}$ which corresponds to a possible increase of the plant inputs (I_{SV1} and I_{SV2}) up to 10 times nominal value. However, simulation results show only for very short time periods (ms) an excess of the nominal servo valve currents. The controller is of order 34 (system rank 32 and 2 further entries due to the weighting matrices W_S and W_T) and is added to the nonlinear system to analyse overshoot, settling time and disturbance rejection of the closed loop system.

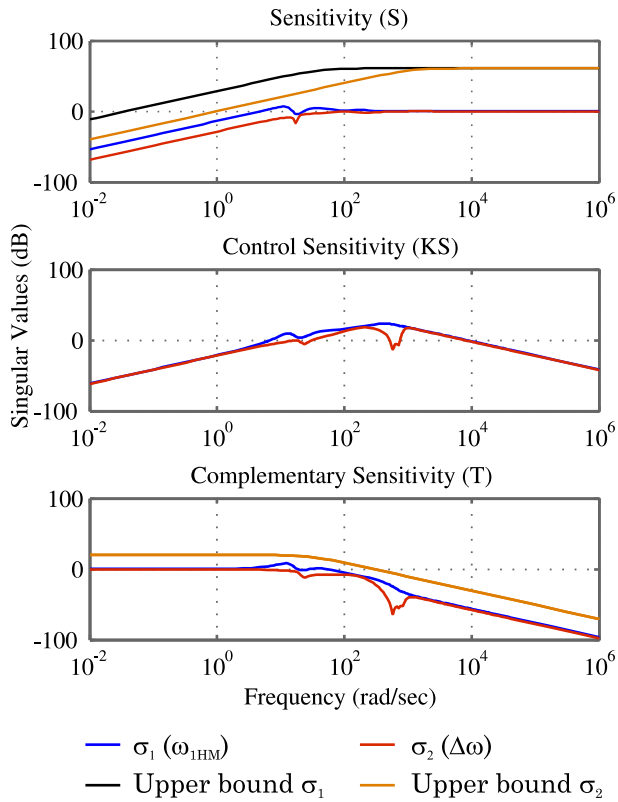

Fig. 9 Singular values σ_1 and σ_2 of S/KS/T

5 Comparison of the Cascade and the Multivariable Controller

In order to compare a set point profile for the simulation and measurement results is defined: the motor speed is commanded to $\omega = 300\,\text{rad/s}$ after $0.5\,\text{s}$. After a time of $2.5\,\text{s}$, a disturbance step to 100kN (50 % of nominal loads) is induced to analyse the disturbance rejection.

5.1 Reference and Disturbance Reactions

Both, the cascade step response and the multi variable controller step response of the motor speed are plotted in figure 10. The step response of the H_∞ controller design reaches the final value faster ($t_{s,H_\infty} = 0.64\,\text{s}$, $t_{s,c} = 1.6\,\text{s}$) with only little overshoot ($\omega_{max,H_\infty} = 302\,\text{rad/s}$, $\omega_{max,C} = 314\,\text{rad/s}$). The speed undershoot in case of applied airload is smaller, using the H_∞ controller design ($\omega_{min,H_\infty} = 200\,\text{rad/s}$, $\omega_{min,C} = 148\,\text{rad/s}$). Moreover the transient time of the H_∞ controller is shorter than the transient time of the cascade ($t_{t,H_\infty} = 0.13\,\text{s}$, $t_{t,c} = 1.04\,\text{s}$). Concluding, the multivariable controller combines a shorter settling time with equivalent overshoot and a better disturbance rejection, compared to the cascade controller concept. Additionally, the control of the motor speed difference yields synchronization of the drive chains in case of differing system parameters.

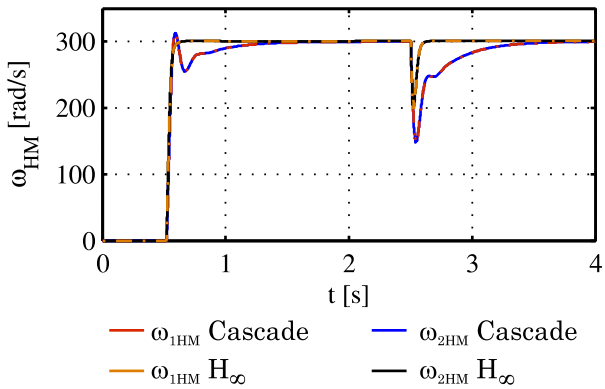

Fig. 10 Simulation results of the motor speed ω_{HM} of the cascade and multivariable controller concept

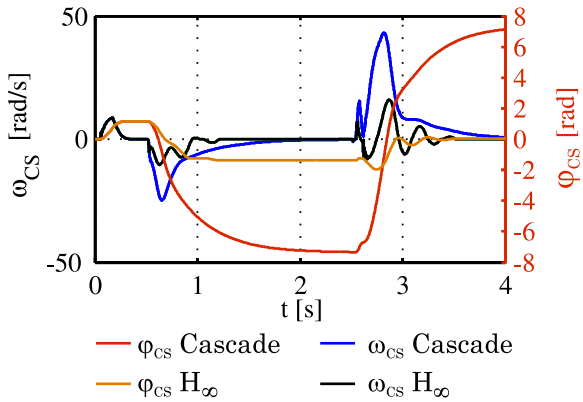

Fig. 11 Cross shaft speed ω_{CS} and angle φ_{CS} in case of different friction parameters

5.2 Drive Chain Synchronization

The synchronization quality can be rated by comparing the movement of the cross shaft for both controller design concepts. In figure 11 the cross shaft movement in case of higher friction torque, affecting the first motor, is plotted. The THSA is accelerated after a time of $0.5\,\text{s}$ to a rotational speed of $300\,\text{rad/s}$. Because of the higher friction torque parameter in the first drive chain, the acceleration phase of the first motor (cascade control concept) takes longer which leads to a cross shaft movement. The cascade controller cannot influence this speed difference until reaching the final value after $2\,\text{s}$, indicated by the stopping of the cross shaft. The H_∞ controller prevents the cross shaft movement after a time period of $1\,\text{s}$ which means that the controller interacts between the two drive chains. At time $2.5\,\text{s}$ a speed of $-300\,\text{rad/s}$ is commanded to both motors. The cross shaft rotation is nearly restricted by the H_∞ controller contrary to the cascade control concept. As the plots in figure 11 show, different system parameter lead to a movement of the cross shaft and consequently to permanent bending stresses in the stabilizer structure. The presented H_∞ controller approach synchronizes the drive chains in nominal operation and therefore prevents fatigue at the linkage of ballscrew and stabilizer structure.

5.3 Discussion and Prospects

The major disadvantage of this H_∞ controller design is the large order ($r_C = 34$) of the controller. It is nearly impossible to implement a controller of order 34 into an actuator control electronic (ACE). There has to be made a trade off between controller complexity (order) and gained performance advantages (shorter settling time, little overshoot, etc.). One possible solution could be to make a full order approach and reduce the controller order afterwards. The H_∞ method provides a stand alone multivariable controller synthesis whereby robustness, disturbance influences and dynamical performance of the control loop are influenced by weighting matrices. A robust controller design with the help of a bounded uncertainties model and an approach to reduce controller complexity, in order to obtain an in-hardware suitable controller, will be continued with the help of the gained experience with the mixed sensitivity controller design for the THSA presented here.

6 Conclusion

This article presents a H_∞ mixed sensitivity controller design approach for a trimmable horizontal stabilizer actuator with two primary load paths. The high order linear state space model and the weighting matrices W_S and W_T are used to calculate the generalized plant and to compute the high order H_∞ controller.

The obtained controller shows in simulation improved performance in overshoot, settling time and disturbance rejection compared to the conventional cascade controller structure. Additionally, the multivariable controller presents a control system solution to synchronize the rotational speeds of the two drive chains, because the speed difference of the hydraulic motors is used as an input signal to the controller. In a continuative approach norm bounded uncertainties will lead to a robust multivariable controller design for the THSA.

Simulation results are validated by measurement results generated with the THSA test rig whose set up is explained here. Measurement results are used to verify the mechanical synchronization of the two load paths in case of different motor speeds e.g. in failure case. The quality of the synchronization (load share) depends directly on the gearing losses and the friction torque affecting the cross shaft.

Acknowledgement

The THSA project was supported by the third national German research program (LUFO III). The investigation of the THSA with two primary load paths takes place in co-operation with LIEBHERR AEROSPACE LINDENBERG GMBH , AIRBUS DEUTSCHLAND GMBH and DLR BRAUNSCHWEIG .

References

[1] Boyd S.P. Balakrishnan V and Kabamba P. A bisection method for computing the H_∞ norm of a transfer function matrix and related problems. *Proc Math. Control Signals Syst. 2*, pp 207–219, 1989.

[2] Föllinger O. *Regelungstechnik*. 8. edition, Hüthig, Heidelberg, Germany, 1994.

[3] Green M. H_∞ controller synthesis by J-lossless coprime factorization. *SIAM Journal on control and Optimazation*, Vol. 30, pp 522–547, 1992.

[4] Müller H. *Die Umlaufgetriebe:Auslegung und vielseitige Anwendung*. Springer, Berlin, Germany, 1998.

[5] Raisch J. *Mehrgrössenregelung im Frequenzbereich*. Oldenbourg, Munich, Germany, 1993.

[6] Skogestad S and Postlethwaite I. *Multivariable Feedback Control*. John Wiley & Sons, Chichester, England, 2005.

[7] Wachendorf N. Carl U and Thielecke F. Model-based failure detection of a trimmable horizontal stailizer actuator with two primary load paths. *Proc 1st CEAS European Air and Space Conference*, pp 1199–1208, Berlin, Germany, 2007.

[8] Zhou K and Doyle J. *Essentials of robust control*. Prentice Hall, 1998.

Copyright Statement

The authors confirm that they, and/or their company or institution, hold copyright on all of the original material included in their paper. They also confirm they have obtained permission, from the copyright holder of any third party material included in their paper, to publish it as part of their paper. The authors grant full permission for the publication and distribution of their paper as part of the ICAS2008 proceedings or as individual off-prints from the proceedings.